

The structural, thermodynamical, elastic, and vibrational properties of LaBi

This article has been downloaded from IOPscience. Please scroll down to see the full text article.

2008 J. Phys.: Condens. Matter 20 345202

(<http://iopscience.iop.org/0953-8984/20/34/345202>)

View [the table of contents for this issue](#), or go to the [journal homepage](#) for more

Download details:

IP Address: 129.252.86.83

The article was downloaded on 29/05/2010 at 13:56

Please note that [terms and conditions apply](#).

The structural, thermodynamical, elastic, and vibrational properties of LaBi

Y O Ciftci^{1,3}, K Colakoglu¹ and E Deligoz²

¹ Department of Physics, Gazi University, Teknikokullar, 06500, Ankara, Turkey

² Department of Physics, Aksaray University, 68100, Aksaray, Turkey

E-mail: yasemin@gazi.edu.tr

Received 2 April 2008, in final form 10 June 2008

Published 1 August 2008

Online at stacks.iop.org/JPhysCM/20/345202

Abstract

In this study, we have studied the structural, elastic, electronic, thermodynamical, and vibrational properties of LaBi by performing *ab initio* calculations within the local-density approximation (LDA). In particular, the lattice constant, bulk modulus, cohesive energy, phase transition pressure (P_t) from the NaCl (B1) to the CsCl (B2) structure, second-order elastic constants (C_{ij}), electronic band structures, and lattice dynamical properties were calculated and compared with the available experimental and other theoretical values. In order to obtain further information, we have also predicted Young's modulus (E), Poisson's ratio (ν), the anisotropy factor (A), sound velocities, Debye temperature (θ_D), and their pressure-dependent behaviour in the B1 phase. In addition, we have estimated the temperature-dependent behaviour of some thermodynamical properties, such as entropy and heat capacity from the lattice dynamical data.

(Some figures in this article are in colour only in the electronic version)

1. Introduction

Lanthanum monopnictides have attracted increased attention because of their scientific and technological importance. It is of significance to understand their various unusual structural, dynamical, electronic, and magnetic properties. The nature of the f electrons in these compounds, which are responsible for magnetic and electrical properties, can be changed from localized to itinerant, leading to significant changes in the structural, physical, and chemical properties of these compounds [1]. The rare-earth pnictides, generally, have low carrier, strongly correlated systems [2], and they show dense Kondo behaviour and heavy fermion states [3–5].

Structurally, LaBi crystallizes in cubic NaCl structure at ambient pressure [6] like other La monopnictides, and at high pressure it undergoes a phase transition either to CsCl (B2) or to tetragonal (BCT) structure [7, 8]. In the B1 phase, the lanthanum atom is positioned at (0, 0, 0) and the bismuth atom at (1/2, 1/2, 1/2) with space group $Fm\bar{3}m$ (225). Although much work has been performed on the lanthanum monopnictides ([6–19], and references therein), LaBi, in the same family, has been the subject of only a few theoretical works [6–10]. Specifically, Davidov *et al*

[6] have measured the lattice constants of rare-earth mono bismuths including LaBi. Vaitheeswaran *et al* [7] have studied the electronic structures and high-pressure structural phases of LaSb and LaBi by using the tight-binding linear muffin tin orbital method (TB-LMTO). These authors analysed the relative stabilities of LaSb and LaBi at high pressures in the rocksalt, primitive tetragonal, and CsCl structures. They concluded that the tetragonal phase rather than the CsCl phase has been preferred. Pagare *et al* [8] have studied the pressure induced structural phase transition and elastic constants of some rare-earth monopnictides including LaBi by using the interatomic potential model. Hasegawa [9] has studied the structural and electronic properties of LaSb and LaBi based on the first-principles methods, and predicted that a BCT phase is stable at high pressure. Benedict [10] has reported the bulk modulus of LaBi in the B1 phase.

However, the other physical properties of this compound have received less or no attention. To our knowledge, the lattice dynamical behaviours, important bulk properties for solids, have been obtained neither theoretically nor experimentally for LaBi so far. Consequently, the main purpose of this work is to provide some information additional to the existing data on the physical properties of LaBi by using the *ab initio* total energy calculations. In particular, we have estimated the melting temperature, phonon dispersion curves, Young's

³ Author to whom any correspondence should be addressed.

Table 1. Calculated equilibrium lattice constant (a_0), bulk modulus (B), the pressure derivative of bulk modulus (B'), and cohesive energy (E_{coh}), together with the theoretical and experimental values for LaBi.

Material	Reference	a (Å)	B (GPa)	B'	E_{coh} (kJ mol ⁻¹)
LaBi (B1)	Present	6.534	62.209	3.409	-1989.3
	Theory ^a	6.392	65.180		
	Theory ^c	6.584	50.03	5.46	-1859.9
	Experimental	6.564 ^a	55.00 ^b		
LaBi (B2)	Present	3.971	65.466	3.59	-1927.9
	Theory ^c	3.968			-1807.5

^a Reference [6].^b Reference [7].^c Reference [8].

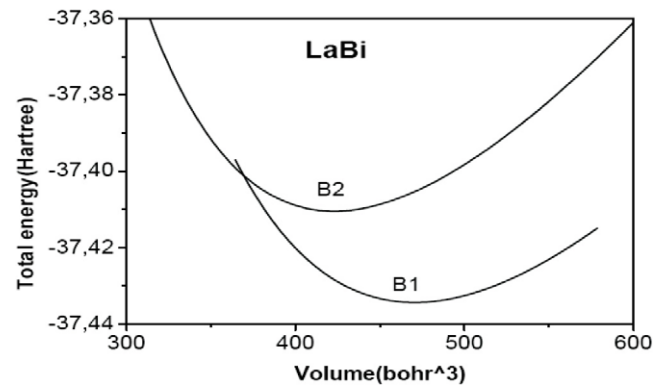
modulus, Poisson's ratio, anisotropy factor, sound velocities, and Debye temperature for LaBi. The pressure dependence of the elastic moduli and the temperature dependence of some thermodynamical properties such as entropy and heat capacity, are also reported, as we have done recently for some lanthanum monopnictides [18, 19]. Calculations on the other basic properties in the B1 phase, such as the lattice constant, bulk modulus, and elastic constants are repeated and compared with the recent theoretical works. The layout of this paper is given as follows: the method of calculation is given in section 2; the results and overall conclusion are presented and discussed in section 3.

2. Method of calculations

The SIESTA (The Spanish Initiative for Electronic Simulations with Thousands of Atoms) code [20, 21] was utilized in this study to calculate the energies and atomic forces. It solves the quantum mechanical equation for the electrons within the density functional approach in the local-density approximation (LDA) For the LDA, the exchange–correlation functional of Ceperley and Adler [22] as parametrized by Perdew and Zunger [23] was used. The interactions between electrons and core ions are simulated with separable Troullier–Martins [24] norm-conserving pseudopotentials. The basis set is based on the finite-range pseudoatomic orbitals (PAOs) of the Sankey–Niklewski type [25], generalized to include multiple-zeta decays.

We have generated atomic pseudopotentials separately for atoms La and Bi by using the $5s^25p^6$ and $6s^26p^3$ atomic configurations, respectively. The basis set for La is $5s$ and $5p$ as semicore (simple zeta). The $6s$ and $5d$ orbitals are described with double-zeta, and a simple-zeta $6p$ is used as polarization for La. The cut-off radii for the present atomic pseudopotentials are taken as s : 1.85, p : 2.20, d : 3.10, f : 1.40 au for La and 2.67 au for the s , p , d and f channels for Bi.

Here, we have used a double-zeta plus polarization (DZP) orbitals basis in which polarization orbitals are constructed from perturbation theory, and they are defined so they have the minimum angular momentum l such that there are no occupied orbitals with the same l in the valence shell of the ground-state atomic configuration. By using the cut-off energies between 100 and 300 Ryd with various basis sets, we found an optimal value of around 150 Ryd. Atoms were allowed to

**Figure 1.** Energy versus volume curves of LaBi.

relax until atomic forces were less than $0.04 \text{ eV } \text{Å}^{-1}$. For the final convergence, 196 k -points were enough to obtain the converged total energies ΔE to about 1 meV/atom for the present compound. The relativistic effects are taken into account for La due to its heavy mass in pseudopotential calculations.

3. Results and discussion

3.1. Structural and electronic properties

First, the equilibrium lattice parameter, bulk modulus, and its pressure derivative are computed by minimizing the crystal's total energy by means of Murnaghan's equation of state (EOS) [26] and are shown in figure 1. The obtained results are also indicated in table 1 along with the other theoretical [6, 8] and experimental [6, 27] values for the B1 and B2 structures. The calculated lattice constant (a_0) and bulk modulus are in excellent agreement with the experimental values for the B1 structure [6, 27] and the agreement is better than some other theoretical findings. It is known that the LDA calculations, generally, underestimate the lattice constants (about 1–2%) and overestimate the bulk modulus (10–12%) as in the present case.

The cohesive energy is known as a measure of the strength of the forces, which bind atoms together in the solid state. The cohesive energy (E_{coh}) of a given phase is defined as the difference in the total energy of the constituent atoms at infinite

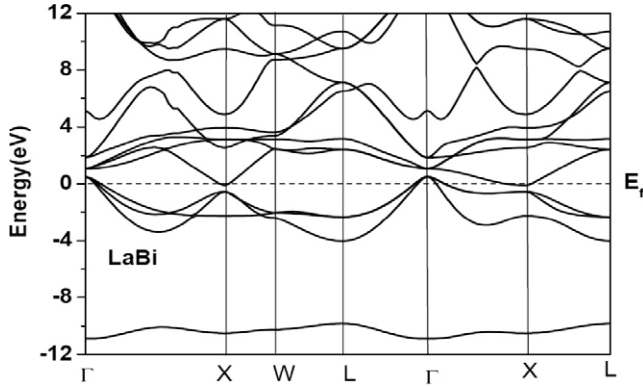


Figure 2. Calculated band structures for LaBi compound in the B1 structure. The position of the Fermi level is at 0 eV.

separation and the total energy of that particular phase:

$$E_{\text{coh}}^{\text{AB}} = [E_{\text{atom}}^{\text{A}} + E_{\text{atom}}^{\text{B}} - E_{\text{total}}^{\text{AB}}]$$

where $E_{\text{total}}^{\text{AB}}$ is the total energy of the compound at the equilibrium lattice constant and $E_{\text{atom}}^{\text{A}}$ and $E_{\text{atom}}^{\text{B}}$ are the atomic energies of the pure constituent atoms. The energy calculations for both pure constituent atoms and compound have to be performed at the same level of accuracy so as to obtain a precise value for the cohesive energy [30]. Energy of an isolated atom is calculated by considering a supercell containing an isolated atom. This is achieved by using the spin-dependent form of functional, with atoms in the ground-state spin configuration.

In this connection, the cohesive energies of LaBi in the B1 and B2 structures are calculated. The computed cohesive energies (E_{coh}) for B1 structures are found to be -1989.3 and -1927.9 kJ mol $^{-1}$ for LaBi in B1 and B2 structures, respectively, and they are also listed in table 1. The present value of E_{coh} is about 7% higher than those given in [8] obtained using the empirical interionic potential method for B1 and B2 structures.

Phase transition pressure from B1 to B2 is only considered and found to be 17.82 GPa in terms of the ‘common tangent technique’ in figure 1.

Although it is not our main intention here to make the detailed band-structure calculations, we have predicted the band structures for LaBi along the high-symmetry directions (see figure 2). They are of comparable quality to the other first-principles LDA calculations [28, 29], and exhibit a metallic character.

3.2. Elastic properties

The elastic constants of solids provide a link between the mechanical and dynamical behaviour of crystals, and give important information concerning the nature of the forces operating in solids. In particular, they provide information on the stability and stiffness of materials, and their *ab initio* calculation requires precise methods. Since the forces and the elastic constants are functions of the first-order and second-order derivatives of the potentials, their

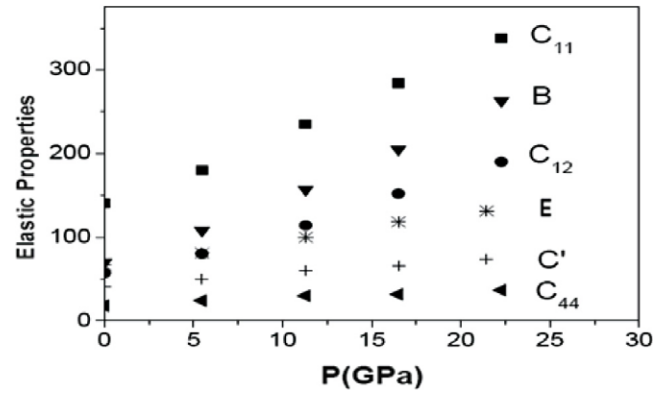


Figure 3. Pressure dependence of elastic properties for LaBi in the B1 structure.

Table 2. Elastic constants (in GPa) for LaBi in the B1 structure.

Material	Reference	C_{11}	C_{12}	C_{44}
LaBi	Present	140.12	58.15	17.94
	Theory ^a	109.6	18.90	18.90

^a Reference [8].

calculation will provide a further check on the accuracy of the calculation of forces in solids. The effect of pressure on the elastic constants is essential, especially, for understanding interatomic interactions, mechanical stability, and phase transition mechanisms. Here, to calculate the elastic constants (C_{ij}), we have used the ‘volume-conserving’ technique [31, 32] as we did recently for LaP and LaAs [18]. The present values of elastic constants for LaBi are given in table 2 along with the other theoretical results for the B1 structure. Our C_{44} value is in accord with the other theoretical value in [8], but the present values of C_{11} and C_{12} are significantly higher than those given in [8] obtained by using the potential model.

The traditional mechanical stability conditions on the elastic constants in cubic crystals are known as $C_{11} - C_{12} > 0$, $C_{11} > 0$, $C_{44} > 0$, $C_{11} + 2C_{12} > 0$, and $C_{12} < B < C_{11}$. Our results for elastic constants given in table 2 satisfy these stability conditions.

We have also calculated the pressure dependence of the second-order elastic constants (SOEC) in the 0–25 GPa pressure range for LaBi, as shown in figure 3. Any experimental data are available for comparison with the figure 3, but similar behaviours were observed in some binary compounds [14, 32]. As expected, both C_{11} and C_{12} increase monotonically with pressure whereas the slope for C_{44} is lower.

The Zener anisotropy factor (A), Poisson’s ratio (ν), shear modulus ($C' = (C_{11} - C_{12})/2$), and Young’s modulus (E), which are the most interesting elastic properties for applications, are also calculated from the computed data using the following relations [33]:

$$A = \frac{2C_{44}}{C_{11} - C_{12}}, \quad (1)$$

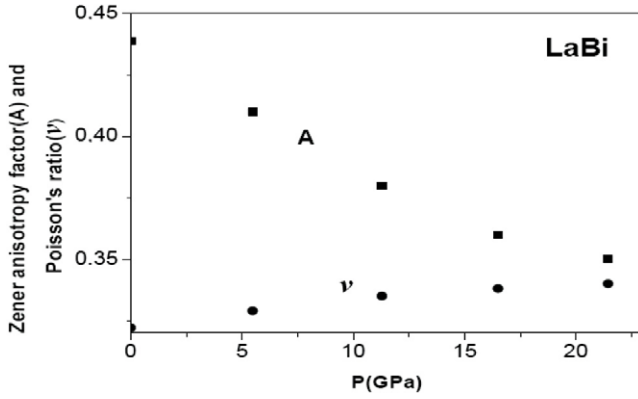


Figure 4. Pressure dependence of Zener anisotropy factor and Poisson's ratio for LaBi in the B1 structure.

Table 3. The calculated Zener anisotropy factor (A), Poisson's ratio (ν), Young's modulus (E), and shear modulus (C') for LaBi in the B1 structure.

Material	Reference	A	ν	E (GPa)	C' (GPa)
LaBi	Present	0.4377	0.3218	66.49	40.98

$$\nu = \frac{1}{2} \left[\frac{(B - \frac{2}{3}G)}{(B + \frac{1}{3}G)} \right], \quad (2)$$

and

$$E = \frac{9GB}{G + 3B} \quad (3)$$

where $G = (G_V + G_R)/2$ is the isotropic shear modulus, G_V is Voigt's shear modulus corresponding to the upper bound of G values, and G_R is Reuss's shear modulus corresponding to the lower bound of G values; they can be written as $G_V = (C_{11} - C_{12} + 3C_{44})/5$, and $5/G_R = 4/(C_{11} - C_{12}) + 3/C_{44}$.

Using the above expressions, we have calculated the values of the Zener anisotropy factor, Poisson's ratio, Young's modulus, and shear modulus for LaBi, as given in table 3. The variations of the anisotropy factor and Poisson's ratio with pressure are also depicted in figure 4. The anisotropy factor at high pressure is important for understanding the evolution of bonding in the system. In figure 4, the anisotropy factor gradually decreases with pressure in the studied pressure range, but the Poisson's ratio shows a small increasing rate, indicating an activation of the shear mode for deformation [34–37]. The variations of Young's and shear moduli with pressure are also depicted in figure 3, and both curves show a similar trend in the considered pressure range. This can be explained by near neighbour replacement of atoms [37–39].

The Debye temperature is known as an important fundamental parameter closely related to many physical properties such as specific heat and melting temperature. At low temperatures the vibrational excitations arise solely from acoustic vibrations. Hence, at low temperatures the Debye temperature calculated from elastic constants is the same as that determined from specific heat measurements. We have calculated the Debye temperature, θ_D , from the elastic constant data by using the average sound velocity, v_m , by the following

Table 4. The longitudinal, transverse, average elastic wave velocity, the Debye temperature and melting temperature for LaBi in the B1 structure.

Material	Reference	v_l (m s ⁻¹)	v_t (m s ⁻¹)	v_m (m s ⁻¹)	θ_D (K)	T_m (K)
LaBi	Present	3398	1741	1950	178	1185 ± 555

common relation given in [40]

$$\theta_D = \frac{\hbar}{k} \left[\frac{3n}{4\pi} \left(\frac{N_A \rho}{M} \right) \right]^{1/3} v_m \quad (4)$$

where \hbar is Planck's constants, k is Boltzmann's constant, N_A is Avogadro's number, n is the number of atoms per formula unit, M is the molecular mass per formula unit, $\rho (= M/V)$ is the density, and v_m is obtained from [41]

$$v_m = \left[\frac{1}{3} \left(\frac{2}{v_l^3} + \frac{1}{v_t^3} \right) \right]^{1/3} \quad (5)$$

where v_l and v_t , are the longitudinal and transverse elastic wave velocities, respectively, which are obtained from Navier's equation [42],

$$v_l = \sqrt{\frac{3B + 4G}{3\rho}} \quad (6)$$

and

$$v_t = \sqrt{\frac{G}{\rho}}. \quad (7)$$

The calculated longitudinal, transverse, and average elastic wave velocities for LaBi are given in table 4. Debye temperature is estimated (average) to be 177.86 K. This value is higher than that for the constituent atom Bi (120 K) and La (142 K) in the β phase.

The empirical relation [43], $T_m = 607 + 9.3B \pm 555$, is used to estimate the melting temperature, and found to be 1185 ± 555 K for LaBi. This value is lower than that for constituent atom La (1193 K) and higher than that for constituent atom Bi (544 K).

3.3. Phonon dispersion curves

The present LDA phonon dispersion curves and density of states of LaBi along the high-symmetry directions were calculated by using the PHONON software [44]. This code, which is compatible with SIESTA, uses the 'Direct Method' [45] and the Hellmann–Feynman forces on atoms for generating the phonon dispersion and the density of states (DOS), and its theoretical and applicational details can be found in [46, 47] and references therein. Specifically, we have calculated the phonon dispersion curves in high-symmetry directions and the DOS for a $2 \times 2 \times 2$ cubic supercell with 64 atoms. The displacement amplitudes are taken as 0.03 Å, and the positive and negative atomic displacements along the x , y , and z directions are taken into account. The Hellmann–Feynman forces acting on the atoms in the supercell are evaluated to construct the force constants and dynamical

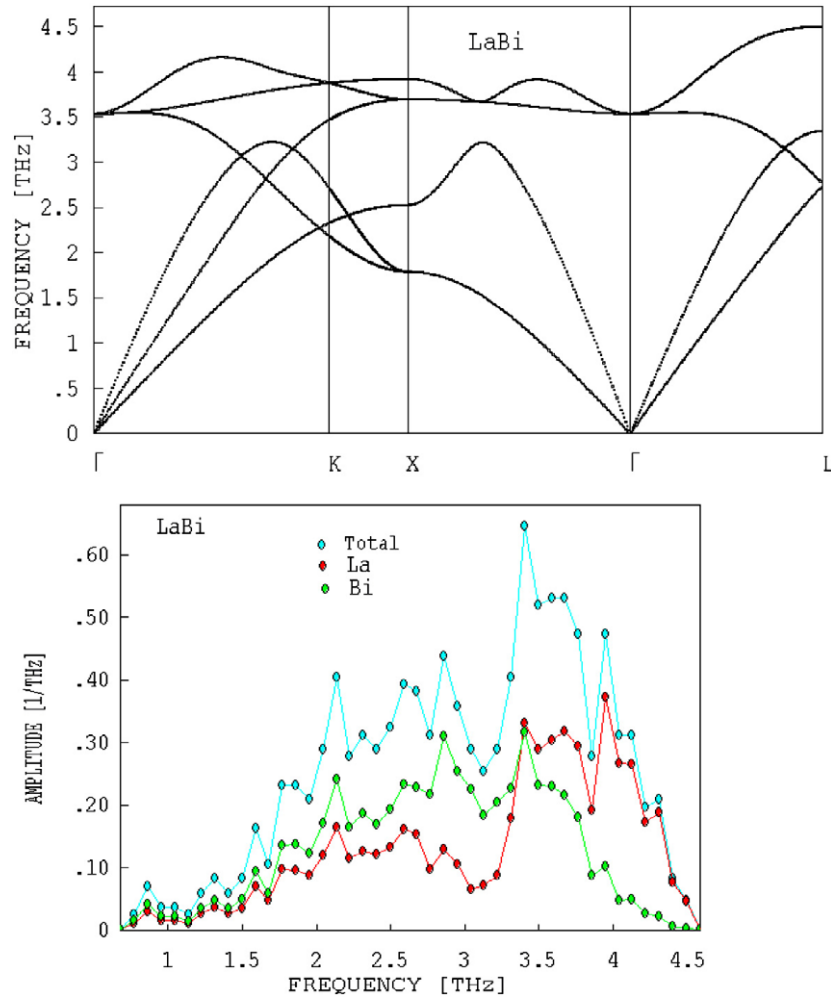


Figure 5. Calculated phonon dispersions, total, and partial density of states for LaBi in the B1 structure.

matrix. Many of the physical properties of solids depend on their phonon properties, such as specific heat, thermal expansion, heat conduction, and electron–phonon interaction.

The obtained phonon dispersion curves and the corresponding one-phonon density of states for LaBi along the high-symmetry directions are illustrated in figure 5. It can be seen from figure 5 that the mass difference between anions and cations seriously affects the shapes of the dispersion curves and the corresponding density of states. For LaBi, the clear gap between the acoustic and optic branches is not seen and they cross in the [110] and [111] symmetry directions. The present phonon dispersion curves are similar to other lanthanum monpnictides such as LaAs and LaP [18] in B1 structure.

The related total and partial densities of phonon states for this compound are shown below the phonon dispersion curves. One can see that the main contribution to acoustic phonons comes from the bismuth sublattice, while the high-frequency phonons are dominated by the La ions.

The data from the partial and total densities of states were used to calculate the temperature dependence of the heat capacity and entropy in the harmonic approximation. We have also plotted the temperature-dependent variations of the

entropy and heat capacity (C_v), at constant volume in the B1 structure for this compound and its constituent atoms, by using the data obtained from SIESTA and PHONON codes [44], in figures 6 and 7. The contributions from the lattice vibration to the total heat capacity of LaBi are illustrated in figure 6. The temperature is limited to 1000 K to decrease the probable influence of anharmonicity. The contribution of the lattice to the heat capacity shown in figure 6 follows the Debye model and approaches the Dulong–Petit limit at high temperatures (about room temperature). At high temperature, it can be seen from these figures that the total heat capacity for LaBi is approximately equal to the sum of the heat capacities of the constituent atoms. The variation of entropy with temperature for LaBi is given in figure 7 over the same temperature range, the total and partial entropy graphs exhibit a similar trend.

As an overall conclusion, we present the results of our calculations, employing the Siesta method, on the structural, mechanical, elastic, electronic, and thermodynamical properties for LaBi. Specifically, the lattice constants, bulk modulus, the pressure derivative of bulk modulus, cohesive energy, elastic constants (and their related quantities, such as Young’s modulus, anisotropy factor, and Poisson’s ratio), pressure dependence of elastic constants, the melting

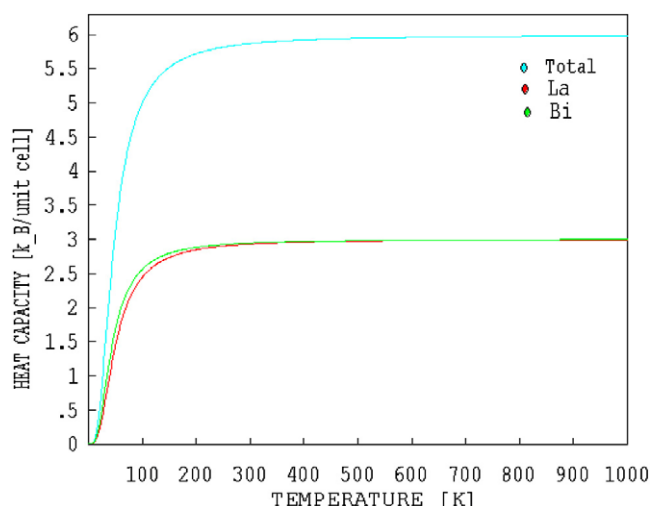


Figure 6. Temperature dependence of heat capacity for LaBi in the B1 structure.

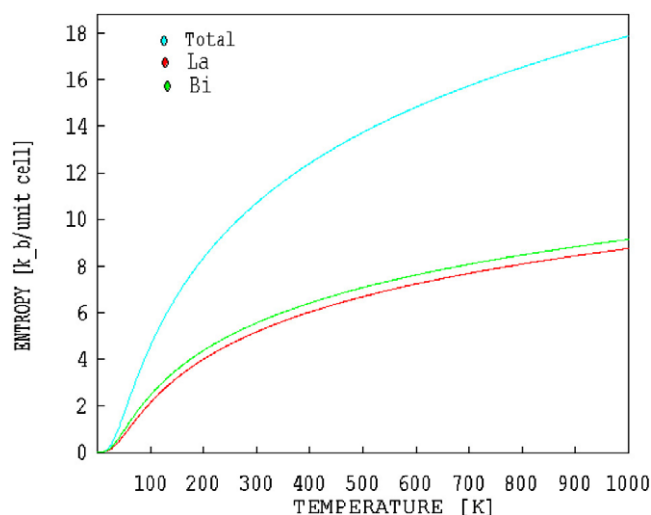


Figure 7. Temperature dependence of entropy for LaBi in the B1 structure.

temperature, the Debye temperature, and phonon frequencies for LaBi have been calculated. The present results are in agreement with the available experimental data and other theoretical findings. The original aspects of the present calculations have been the phonon dispersion curves, mechanical properties, and thermodynamical results, which have not been considered previously. We hope that some of our results will be tested, to confirm the reliability, experimentally and theoretically using different methods.

Acknowledgments

This work is supported by the Gazi University Research Project Unit under project No. 05/2007-23. We also wish to thank the referees for useful suggestions and comments.

References

- [1] Chandra S N V and Sahu P Ch 2006 *J. Mater. Sci.* **41** 3207
- [2] Li D X, Haga Y, Shida H, Suzuki T and Kwon Y S 1996 *Phys. Rev. B* **54** 10483
- [3] Yoshida M, Koyama K, Sakon T, Ochiai A and Motokawa M 2000 *J. Phys. Soc. Japan* **69** 3629
- [4] Yoshida M, Koyama K, Ochiai A and Motokawa M 2005 *Phys. Rev. B* **71** 75102
- [5] Adachi T, Shirotani I, Hayashi J and Shimomura O 1998 *Phys. Lett. A* **250** 389
- [6] Davidov D, Bucher E, Rupp L W, Longinotti D and Rettori C 1974 *Phys. Rev. B* **9** 2879
- [7] Vaitheeswaran G, Kanchana V and Rajagopalan M 2002 *Physica B* **315** 64
- [8] Pagare G and Sanyal S P 2006 *Phase Transit.* **79** 935
- [9] Hasegawa A 1985 *J. Phys. Soc. Japan* **54** 677
- [10] Benedict U 1995 *J. Alloys Compounds* **223** 216
- [11] Pagare G, Sanyal S P and Jha P K 2005 *J. Alloys Compounds* **398** 16
- [12] Hasegawa A 1980 *J. Phys. C: Solid State Phys.* **13** 6147
- [13] Shirotani I, Yamanashi K, Hayashi J, Ishimatsu N, Shimomura O and Kikegawa T 2003 *Solid State Commun.* **127** 573
- [14] Bouhemadou A, Khenata R and Maamache M 2006 *J. Mol. Struct. Theochem.* **777** 5
- [15] Yoshida M, Koyama K, Ochiai P A and Motokawa M 2005 *Phys. Rev. B* **71** 75102
- [16] Kaneta Y, Sakai O and Kasuya T 1993 *Physica B* **186** 156
- [17] Tütüncü H M, Bağcı S and Srivastava G P 2007 *J. Phys.: Condens. Matter* **19** 156207
- [18] Deligöz E, Çolakoğlu K, Çiftçi Y Ö and Ozisik H 2007 *J. Phys.: Condens. Matter* **19** 436204
- [19] Ciftci Y O, Çolakoğlu K, Deligöz E and Ozisik H 2008 *Mater. Chem. Phys.* **108** 120
- [20] Ordejón P, Artacho E and Soler J M 1996 *Phys. Rev. B* **53** 10441 (Rapid Comm.)
- [21] Soler J M, Artacho E, Gale J D, García A, Junquera J, Ordejón P and Sánchez-Portal D 2002 *J. Phys.: Condens. Matter* **14** 2745
- [22] Ceperley D M and Alder M J 1980 *Phys. Rev. Lett.* **45** 566
- [23] Perdew P and Zunger A 1981 *Phys. Rev. B* **23** 5048
- [24] Troullier N and Martins J L 1991 *Phys. Rev. B* **43** 1993
- [25] Sankey O F and Niklewski D J 1989 *Phys. Rev. B* **40** 3979
- [26] Murnaghan F D 1944 *Proc. Natl Acad. Sci. USA* **30** 5390
- [27] Benedict U, Dabos-Seignon S, Dancausse J P, Gensini M, Gerward L and Haire R G 1992 *J. Alloys Compounds* **181** 1
- [28] Vaitheeswaran G, Kanchana V and Rajagopalan M 2002 *Physica B* **315** 64
- [29] Pagare G, Sanyal S P and Jha P K 2005 *J. Alloys Compounds* **398** 16
- [30] Ahmed R, Hashemifar S J, Akbarzadeh H, Ahmed M and Alem F 2007 *Comput. Mater. Sci.* **39** 580
- [31] Wang S Q and Ye H Q 2003 *Phys. Status Solidi b* **240** 45
- [32] Mullen M E, Lüthi B, Wang P S, Bucher E, Longinotti L D and Maita J P 1974 *Phys. Rev. B* **10** 186
- [33] Mayer B, Anton H, Bott E, Methfessel M, Sticht J and Schmidt P C 2003 *Intermetallics* **11** 23
- [34] Fukuhara M and Yamauchi I 1993 *J. Mater. Sci.* **28** 4681
- [35] Fukuhara M and Sanpei S 1993 *Iron Steel Inst. Japan Int.* **33** 508
- [36] Fukuhara M and Sanpei S 1993 *Idem. J. Mater. Sci. Lett.* **12** 1122
- [37] Fukuhara M, Sanpei A and Shibuki K 1997 *J. Mater. Sci.* **32** 1207
- [38] Deeg E 1958 *Glasstech. Ber.* **31** 124
- [39] Spinner S and Cleek G W 1960 *J. Appl. Phys.* **31** 1407
- [40] Christman J R 1988 *Fundamentals of Solid State Physics* (New York: Wiley)

- [41] Anderson O L 1963 *J. Phys. Chem. Solids* **24** 909
- [42] Scriber E, Anderson O L and Soga N 1973 *Elastic Constants and their Measurements* (New York: McGraw-Hill)
- [43] Johnston I, Keeler G, Rollins R and Spicklemire S 1996 *Solid State Physics Simulations, The Consortium for Upper-Level Physics Software* (New York: Wiley)
- [44] Parlinski K 2003 *Software Phonon* and references therein
- [45] Parlinski K, Li Z Q and Kawazoe Y 1997 *Phys. Rev. Lett.* **78** 4063
- [46] Parlinski K, Łazewski J and Kawazoe Y 2000 *J. Phys. Chem. Solids* **61** 87
- [47] Parlinski K 2005 *Mater. Sci. Pol.* **23** 357